DOI: 10.1002/ejic.200701124

A Dawson-Type Dirhenium(V)-Oxido-Bridged Polyoxotungstate: X-ray Crystal Structure and Hydrogen Evolution from Water Vapor under Visible Light Irradiation

Chika Nozaki Kato,*[a] Kazunobu Hara,[a] Ayumi Hatano,[b] Kazuhiro Goto,[b] Tomonori Kuribayashi,[b] Kunihiko Hayashi,[b] Akira Shinohara,[b] Yusuke Kataoka,[b] Wasuke Mori,[b] and Kenji Nomiya[b]

Keywords: Polyoxometalates / Rhenium / X-ray diffraction / UV/Vis spectroscopy / Photocatalysis

The synthesis and crystal structure of a Dawson-type dirhenium(V)-oxido-bridged polyoxotungstate are described. The potassium salt $K_{14}[O\{Re^{V}(OH)(\alpha_2\text{-}P_2W_{17}O_{61})\}_2]\cdot 21H_2O$ (K-**1**) was obtained as analytically pure, homogeneous, black-purple crystals by the reaction of a monolacunary Dawson polyoxotungstate with $[Re^{IV}Cl_6]^{2-}$ in water, followed by crystallization from an aqueous HCl solution in the dark. Single-crystal X-ray structure analysis revealed that the dimeric dirhenium(V)-oxido-bridged structure has overall C_{2h} symmetry. Characterization of K-**1** was also accomplished by elemental analysis, TG/DTA, and FTIR, UV/Vis absorption, ESR, and solution ^{31}P NMR spectroscopy. Furthermore, the black-purple compound K-**1** was grafted onto a TiO_2 surface by electrostatic binding to give TiO_2 with a cationic quaternary ammonium moiety (**1**-grafted TiO_2). Elemental analysis of **1**-grafted TiO_2 indicated that the seven potassium counterions of K-**1** were ion-exchanged with seven cationic ammonium moieties to form $\{TiO_2\}_{5500}[\equiv Si(CH_2)_3N(CH_3)_3Cl]_7[\equiv Si(CH_2)_3\text{-}N^{+}(CH_3)_3]_7(K_7[O\{Re(OH)(\alpha_2\text{-}P_2W_{17}O_{61})\}_2]^{7-})$ and seven molecules of KCl. The diffuse reflectance (DR) UV/Vis spectrum of **1**-grafted TiO_2 exhibited two sharp bands at 496 nm and 751 nm due to the $Re^{V}\rightarrow W^{VI}$ intervalence charge transfer (IVCT) band and the d–d band of the rhenium(V) atom, respectively, in the visible light region, which suggested that polyoxoanion **1** was isolated on the TiO_2 surface. With **1**-grafted TiO_2, hydrogen evolution from water vapor under irradiation with visible light (>400 nm and >420 nm) was achieved.

Introduction

The construction of an efficient device for the photosplitting of water to hydrogen is one of the most important subjects from the viewpoint of solar light energy utilization and storage since Honda and Fujishima first demonstrated a photoelectrochemical cell consisting of a TiO_2 photoanode and a Pt cathode to decompose water into hydrogen and oxygen under ultraviolet (UV) irradiation with an external bias.[1] The design and preparation of new photocatalysts that are responsive in a similar manner to visible light are a key target for the utilization of solar energy for hydrogen production. To develop efficient photocatalysts that work under visible light irradiation, a number of attempts have been made, e.g., a chemically modified n-type TiO_2 by controlled combustion of Ti metal in a neutral gas flame (this material absorbs light at wavelengths below 535 nm),[2] visible-light-response TiO_2 thin films prepared by a radio-frequency magnetron sputtering deposition method,[3] NiO_x (partly oxidized nickel) promoted $In_{0.9}Ni_{0.1}TaO_4$,[4] $(AgIn)_x\text{-}Zn_{2(1-x)}S_2$,[5] and $(Ga_{1-x}Zn_x)(N_{1-x}O_x)$ with RuO_2, transition-metal mixed-oxides containing Cr, and noble-metal/Cr_2O_3 (core/shell) nanoparticles as co-catalysts.[6] These materials are powerful photocatalysts for water splitting under visible light irradiation; however, the search for the use of other materials as visible-light-response photocatalysts is still an interesting objective.

Polyoxometalates (POMs) have attracted considerable attention because of their extreme versatility and unique range of properties, including catalytic and biological activities and/or photochemical, electrochromic, and magnetic properties.[7] However, there is no report regarding the use of POMs as photocatalysts for the water splitting reaction under visible light irradiation. $H_3PW_{12}O_{40}$ encapsulated into the titanium-exchanged HY(TiHY) zeolite required both UV and visible light for the water splitting reaction.[8] To improve the visible light absorption of POMs, we focused on the synthesis of Dawson-type dirhenium(V)-oxido-bridged POM, $[O\{Re^{V}(OH)(\alpha_2\text{-}P_2W_{17}O_{61})\}_2]^{14-}$ (**1**). Then, we prepared a new type of POM-based photocatalyst

[a] Department of Chemistry, Faculty of Science, Shizuoka University,
836 Ohya, Suruga-ku, Shizuoka 422-8529, Japan
Fax: +81-54-237-3384
E-mail: sckatou@ipc.shizuoka.ac.jp
[b] Department of Materials Science, Faculty of Science, Kanagawa University,
Tsuchiya 2946, Hiratsuka, Kanagawa 259-1293, Japan

Supporting information for this article is available on the WWW under http://www.eurjic.org or from the author.

material by the electrostatic grafting of polyoxoanion **1** onto an anatase TiO_2 surface through the cationic ammonium moiety (**1**-grafted TiO_2).

In this paper, we report the full details of the synthesis and characterization of the potassium salt $K_{14}[O\{Re^{V}(OH)(\alpha_2\text{-}P_2W_{17}O_{61})\}_2]\cdot 21H_2O$ (K-**1**) and the **1**-grafted TiO_2 material. Furthermore, the photocatalytic performance of **1**-grafted TiO_2 material in hydrogen formation from water vapor under irradiation with visible light (>400 nm and >420 nm) is investigated.

Results and Discussion

Synthesis, Characterization, and Molecular Structure of a Potassium Salt of the Dawson-Type Dirhenium(V)-Oxido-Bridged POM (K-1)

The potassium salt of compound **1**, $K_{14}[O\{Re^{V}(OH)(\alpha_2\text{-}P_2W_{17}O_{61})\}_2]\cdot 21H_2O$ (K-**1**), was synthesized by a slight modification of the published method for the synthesis of monomeric monorhenium(V)-substituted POM $K_7[\alpha_2\text{-}Re^{V}OP_2W_{17}O_{61}]\cdot 2H_2O$.[9] Compound K-**1** was formed by heating at reflux the mixture of $K_2Re^{IV}Cl_6$ and monolacunary Dawson POM $[\alpha_2\text{-}P_2W_{17}O_{61}]^{10-}$ in an aqueous solution in air followed by reprecipitation from hot water in the dark. The pH of the solution changed from 3.40 to 1.54 during the reaction. The formation of K-**1** is given by the ionic balance shown in Equation (1), in which rhenium(IV) is oxidized to rhenium(V).

$$2\ Re^{IV}Cl_6^{2-} + 2\ [\alpha_2\text{-}P_2W_{17}O_{61}]^{10-} + 3\ H_2O \rightarrow [O\{Re^{V}(OH)(\alpha_2\text{-}P_2W_{17}O_{61})\}_2]^{14-} + 4\ H^+ + 12\ Cl^- \quad (1)$$

The crystallization of K-**1** for the single-crystal X-ray analysis was performed by slow evaporation from an aqueous HCl solution (pH = 1.5) in the dark. Good crystals could not be obtained in water. The X-ray crystallographic structural analysis of K-**1** exhibits a dimeric dirhenium(V)-oxido-bridged structure, as shown in Figure 1. The structure of K-**1** is that of a $(P_2W_{17}Re)_2$-O dimer with a Re–O–Re linkage, which is similar to the structure of Dawson diruthenium(IV)-oxido-bridged POM $[O\{Ru^{IV}(Cl)(\alpha_2\text{-}P_2W_{17}O_{61})\}_2]^{16-}$.[10] Both $\alpha_2\text{-}P_2W_{17}O_{61}{}^{10-}$ units act as tetradentate chelating and bridging ligands to the Re atoms and possess a center of symmetry for the anion. The two sets of four oxygen atoms attached to the Re atoms in a plane perpendicular to the Re(1)–O(1M)–Re(1A) axis are eclipsed to give a C_{2h} symmetry. The length of the Re(1)–O(1M) bond coordinated to the four oxygen atoms in the lacunary site is 1.7690(14) Å, which is smaller than that of Re^{V}–O in O=Re^{V}–O–Re^{V}=O (ca. 1.9 Å)[11] but similar to that in $[O\{Ru^{IV}(Cl)(\alpha_2\text{-}P_2W_{17}O_{61})\}_2]^{16-}$ (1.773 Å) (see Table 1).[10] The Re–O(1H) bond length [2.369(14) Å; *trans* to the Re–O–Re in **1**] is longer than those of the Re^{V}–OH bonds (1.811–1.970 Å) in monomeric complexes of the type $[Re^{V}O(OH)L_4]$ (L = pyridine, CN^-, cyclam, en).[12]

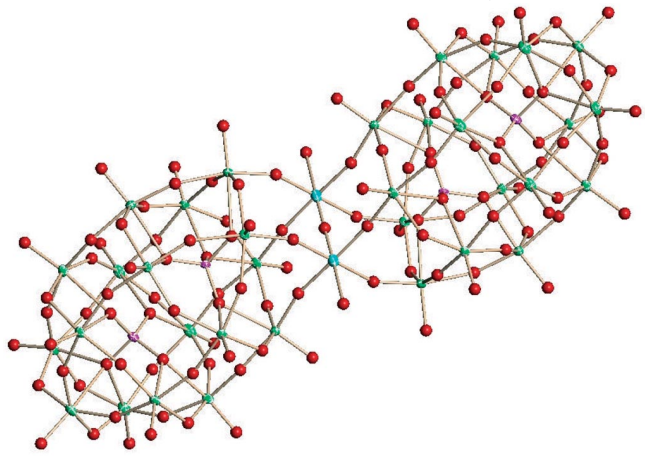

Figure 1. Molecular structure of K-**1** with 50% probability ellipsoids.

Table 1. Selected bond lengths [Å] and angles [°] for K-**1** around the Re–O–Re linkage.

Bond lengths			
Re(1)–O(1M)	1.7690(14)	Re(1)–O(5A)	1.939(17)
Re(1)–O(1H)	2.369(14)	Re(1)–O(9A)	1.917(19)
Re(1)–O(1)	1.942(17)	Re(1)–O(10)	1.951(17)
Bond angles			
O(1M)–Re(1)–O(1H)	178.9(4)	O(9A)–Re(1)–O(1)	90.9(8)
O(1M)–Re(1)–O(1)	90.1(5)	O(1)–Re(1)–O(10)	89.8(7)
O(1M)–Re(1)–O(5A)	90.5(5)	O(9A)–Re(1)–O(5A)	89.1(8)
O(1M)–Re(1)–O(9A)	88.5(5)	O(5A)–Re(1)–O(10)	90.3(7)
O(1M)–Re(1)–O(10)	87.5(5)	O(9A)–Re(1)–O(10)	176.0(7)
O(1)–Re(1)–O(1H)	88.9(6)	W(1)–O(1)–Re(1)	153.6(10)
O(5A)–Re(1)–O(1H)	90.5(6)	W(2)–O(5)–Re(1A)	153.8(10)
O(9A)–Re(1)–O(1H)	92.1(7)	W(6)–O(9)–Re(1A)	167.2(11)
O(10)–Re(1)–O(1H)	91.9(6)	W(7)–O(10)–Re(1)	166.3(10)
O(5A)–Re(1)–O(1)	179.5(8)	Re(1A)–O(1M)–Re(1)	180

The bond valence sum (BVS) value of the Re atom is 5.782; which is in the range 5.556–6.864 that was observed for Re^{V}–O–Re^{V} complexes,[11] above the range of the BVS values observed in Re^{III}–O–Re^{III} complexes (5.298–5.336),[13] but below the range of BVS values observed in Re^{VII}–O–Re^{VII} complexes (7.557–7.920).[14] Therefore, on the basis of Re–oxygen bond lengths, valence sums, bulk diamagnetism, and charge balance from the analytical stoichiometry, we assign the +5 oxidation state to the rhenium atoms. Note also that each Re was clearly 6- and not 7-coordinate, as shown in Figure 1. The BVS values of the 17W atoms are in the range 5.912–6.442 (average: 6.229), and those of the two P atoms are in the range 5.002–5.019 (5.011). These values correspond reasonably well to the formal valances W^{6+} and P^{5+}, respectively (see Tables S1 and S2 in the Supporting Information).

The crystal structure of K-**1** is consistent with the elemental analysis, TG/DTA data, UV/Vis absorption, FTIR, ESR, and solution ^{31}P NMR spectra. The elemental analysis had to be performed for compound K-**1** after drying it at room temperature at 10^{-3}–10^{-4} Torr overnight. The result was consistent with the composition $K_{14}[O\{Re^{V}(OH)(\alpha_2\text{-}$

$P_2W_{17}O_{61})\}_2]\cdot 6H_2O$. The weight loss observed during the course of drying before analysis was 2.8% for K-**1**; this corresponds to 15–16 weakly solvated or adsorbed water molecules. The TG/DTA measurement performed under ambient conditions showed a weight loss of 3.93% without a clear endothermic point; this value corresponds to 21 water molecules including both the intrinsic water of hydration and the water adsorbed from the atmosphere. Thus, the number of hydrated water molecules in compound K-**1** is 21. The elemental analysis of the crystalline sample of K-**1** also showed the same composition as the powder sample and the absence of chloride ion after the crystallization from an aqueous HCl solution.

The FTIR spectrum of compound K-**1** measured by using a KBr disk is shown in Figure 2. The positions of all the bands (1091, 1018, 954, 907, 787, and 526 cm^{-1}) in the polyoxoanion region of this compound are similar to those of $[\alpha\text{-}P_2W_{18}O_{62}]^{6-}$ (1091, 1020, 958, 912, 777, and 528 cm^{-1}) rather than to those of $[\alpha_2\text{-}P_2W_{17}O_{61}]^{10-}$ (1086, 1054, 1016, 940, 885, 811, 741, 601, 527, and 467 cm^{-1}), suggesting the coordination of rhenium atoms by the monovacant site of the $[\alpha_2\text{-}P_2W_{17}O_{61}]^{10-}$.

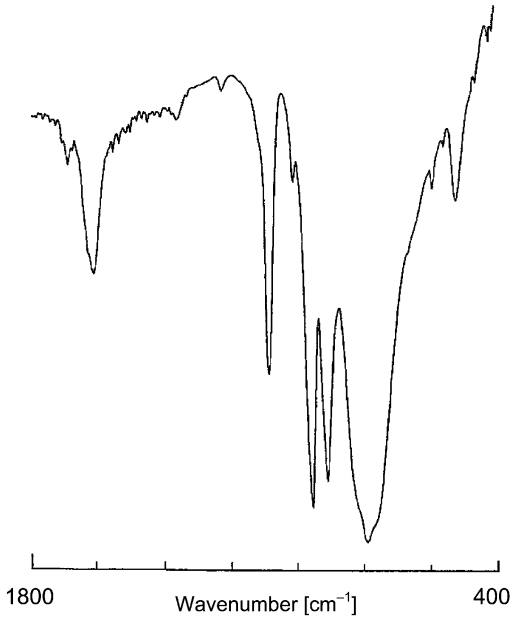

Figure 2. FTIR spectrum, measured by using a KBr disk, in the polyoxoanion region (1800–400 cm^{-1}) of K-**1**.

The ^{31}P NMR spectrum of K-**1** in D_2O at about 25 °C has a clear two-line spectrum at δ = –12.38 and –13.39 ppm (referenced to 25%H_3PO_4) and δ = –12.06 and –13.05 ppm (referenced to 85%H_3PO_4), showing that K-**1** is a diamagnetic compound with an antiferromagnetic interaction between the two Re^V atoms (see Figure 3). The downfield resonance was assigned to the phosphorus closest to the rhenium sites and the upfield resonance to the phosphorus closer to the W_3 cap. These signals exhibit a shift from those of $[\alpha_2\text{-}P_2W_{17}O_{61}]^{10-}$ (δ = –6.96 and –14.10 ppm; referenced to 25%H_3PO_4) and $[\alpha\text{-}P_2W_{18}O_{62}]^{6-}$ (δ = –12.75 ppm; referenced to 25%H_3PO_4), indicating the complete coordination of rhenium atoms by the monovacant site of $[\alpha_2\text{-}P_2W_{17}O_{61}]^{10-}$ and the high purity of K-**1**. It should be noted that the spectral pattern of K-**1** is quite similar to that of the reported monomeric monorhenium(V)-substituted POM $K_7[\alpha_2\text{-}Re^VOP_2W_{17}O_{61}]\cdot 2H_2O$, but the chemical shift was somewhat different from the values of –11.86 and –12.86 ppm (referenced to 85%H_3PO_4) for $K_7[\alpha_2\text{-}Re^VOP_2W_{17}O_{61}]\cdot 2H_2O$. The ^{31}P NMR spectrum of the crystalline sample of K-**1** crystallized from an aqueous HCl solution also showed the same chemical shifts (δ = –12.46 and –13.45 ppm; referenced to 25%H_3PO_4) as those of the powder sample. No ESR signals of solid K-**1** at room temperature were detected over a wide range of magnetic fields, also suggesting that K-**1** is diamagnetic compound.

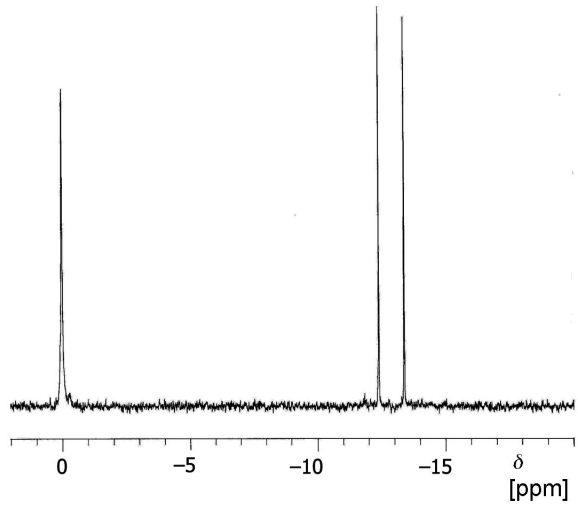

Figure 3. ^{31}P NMR spectrum of K-**1** in D_2O. The resonance at 0.0 ppm is due to the external reference: 25% H_3PO_4 in H_2O.

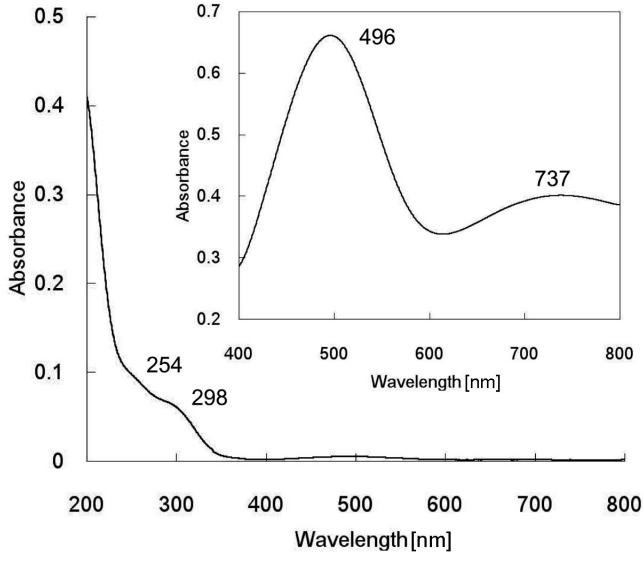

Figure 4. UV/Vis spectrum of K-**1** in H_2O in the range 200–800 nm ($\times 10^{-6}$ M). Inset: in the range 400–800 nm ($\times 10^{-4}$ M).

The UV/Vis spectrum of K-**1** in water has four absorption bands at 254 nm ($\varepsilon = 9.39 \times 10^4$ м$^{-1}$ cm^{-1}), 298 nm ($\varepsilon = 6.28 \times 10^4$ м$^{-1}$ cm^{-1}), 496 nm ($\varepsilon = 6.61 \times 10^3$ м$^{-1}$ cm^{-1}), and 737 nm ($\varepsilon = 4.02 \times 10^3$ м$^{-1}$ cm^{-1}), as shown in Figure 4. Two large bands at 254 nm and 298 nm were assigned to the charge transfer (CT) bands of W–O, and two small bands at 496 nm and 737 nm were assigned to the $Re^{V} \rightarrow W^{VI}$ intervalence charge transfer (IVCT) band and d-d band of the rhenium(V) atom, respectively.[15,16]

Preparation, Characterization, and Photocatalytic Performance of Anatase TiO_2 Functionalized by a Cationic Ammonium Moiety by Impregnation with 1

The black-purple compound K-**1** that was prepared was grafted onto a TiO_2 surface by electrostatic binding to give TiO_2 functionalized with cationic quaternary ammonium groups according to the published method.[17] This material (abbreviated as TiO_2–N^+) was obtained by the addition of a 50% methanol solution of *N*-trimethoxysilylpropyl-*N*,*N*,*N*-trimethylammonium chloride, $(MeO)_3Si(CH_2)_3N^+(CH_3)_3$-Cl, to a TiO_2 suspension in methanol at 25 °C. In this reaction, the methoxy groups of the silane coupling reagent reacted cleanly with the hydroxy groups of TiO_2 to eliminate methanol and form the isolated surface species $\equiv Si(CH_2)_3$-$N(CH_3)_3Cl$. Then, polyoxoanion **1** was grafted onto TiO_2–N^+ by employing the ion-exchange reaction of potassium ion with a cationic ammonium moiety in water at 25 °C. The product obtained is abbreviated as **1**-grafted TiO_2. According to the elemental analysis result, the loading of K-**1** was found to be 2.2 μmol g^{-1} [the amount of the surface cationic quaternary ammonium groups, $\equiv Si(CH_2)_2N(CH_3)_3$-Cl, was 31.7 μmol g^{-1}]. The amount of potassium observed in the elemental analysis of **1**-grafted TiO_2 was 0.032%, indicating that the seven potassium counterions of K-**1** were ion-exchanged with the seven cationic ammonium moieties to form $\{TiO_2\}_{5500}[\equiv Si(CH_2)_3N(CH_3)_3Cl]_7[\equiv Si(CH_2)_3N^+$-$(CH_3)_3]_7(K_7[O\{Re(OH)(\alpha_2\text{-}P_2W_{17}O_{61})\}_2]^{7-})$ and seven molecules of KCl. Thus, 49% of the surface silane coupling reagent of TiO_2–N^+ was covered by the grafting reaction with K-**1**. The byproduct KCl can easily be removed by washing with excess water.

The diffuse reflectance (DR) UV/Vis spectrum of **1**-grafted TiO_2 (2.2 μmol g^{-1}) showed two sharp bands at 496 nm and 751 nm in the visible light region (see Figure 5a), suggesting that the surface species **1** is isolated on the TiO_2 surface.[18] These bands might be assigned to the $Re^{V} \rightarrow W^{VI}$ intervalence charge transfer (IVCT) band and the d–d band of rhenium(V) atom, respectively. The ^{31}P NMR spectrum of solid **1**-grafted TiO_2 was not possible to obtain because of the low loading of **1**. The BET surface area was 39.4 m^2 g^{-1} after the grafting of **1** onto the TiO_2 surface, which was almost the same as that of the starting TiO_2 material (40.0 m^2 g^{-1}).

We initially examined the evolution of H_2 from water vapor under light irradiation greater than 400 nm and 420 nm and catalyzed by **1**-grafted TiO_2 at 25 °C without any additives in heterogeneous systems, as shown in Table 2. The reaction did not proceed when light irradiation was stopped, even at 60 °C. With regard to the time course of H_2 evolution catalyzed by **1**-grafted TiO_2 under light irradiation (>400 nm), a linear increase in H_2 with time was observed, as shown in Figure 6a. After 5 h, the amount of H_2 evolved was 19.8 μmol per g of catalyst [the rate, calculated on the basis of the formula (mol g^{-1} of H_2) h^{-1}, is 3.96 μmol g^{-1} h^{-1}]. After 55 h, the amount of H_2 evolved reached 101.6 μmol per g of catalyst [the turnover number (TON), calculated on the basis of the formula (mol of H_2)/(mol of **1** per g of catalyst), is 46.2] (Table 2, Entry 1). The catalytic activities were reproducible on five repeated runs. 19.5 μmol water vapor remained in the gas phase after 55 h, and some amounts of water vapor were adsorbed on the TiO_2 surface. O_2, CO_2, CO, and CH_4 were not detected under the present reaction conditions. The apparent quantum yield (AQY) was quite low, i.e., <0.1% at 405 nm after 25 h; however, there is no report regarding AQY for H_2

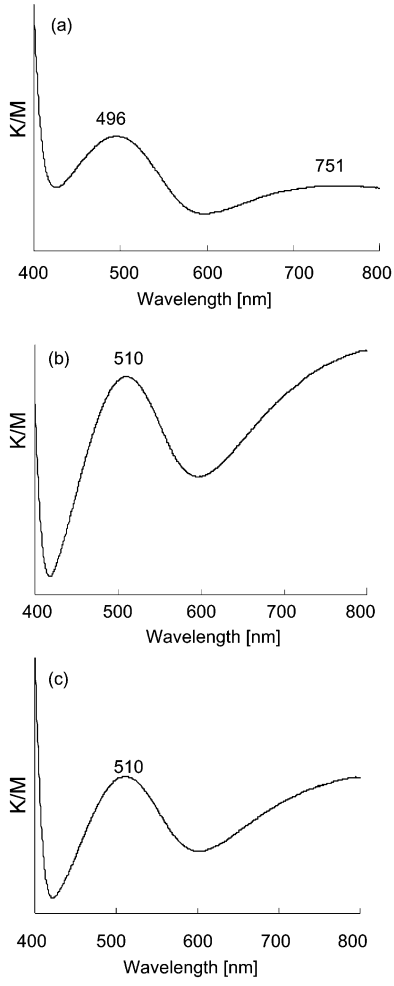

Figure 5. Diffuse reflectance UV/Vis spectra of (a) as-prepared **1**-grafted TiO_2, (b) **1**-grafted TiO_2 after H_2 evolution from water vapor (20 Torr) under irradiation with visible light (>400 nm), and (c) **1**-grafted TiO_2 after H_2 evolution from water (10 mL) in the liquid-phase reaction containing $Na_2H_2EDTA{\cdot}2H_2O$ under irradiation with visible light (>400 nm).

evolution from water vapor without any additives. No H_2 evolution was detected in the absence of water vapor. A mixture of K-**1** (5.6 μmol) and TiO_2 (1.0 g) in the absence of a silane coupling reagent induced 2.98 μmol g^{-1} and 8.52 μmol g^{-1} of H_2 evolution after 25 h and 50 h, respectively (rate: 1.19×10^{-1} μmol g^{-1} h^{-1} after 25 h; TON: 3.9 after 50 h) (Table 2, Entry 2). In addition, the photodecomposition of D_2O vapor (20 Torr) was carried out under light irradiation (>400 nm). D_2, H_2, and HD were detected after 48 h, which were due to the decomposition of D_2O vapor, the decomposition of the surface silane coupling reagent, and the H–D exchange reaction of D_2 with H_2, respectively. These results indicate that H_2 was certainly evolved from water vapor; however, the surface silane coupling reagent of **1**-grafted TiO_2 was also decomposed. Under light irradiation at a wavelength greater than 420 nm, a long induction period was observed (see Figure 6b). After 93 h, the amount of H_2 production was 1.57 μmol g^{-1} of catalyst (rate: 1.69×10^{-2} μmol g^{-1} h^{-1}). After 380 h, the amount of H_2 evolved reached 4.35 μmol g^{-1} of catalyst (TON: 1.98) (Table 2, Entry 3), which was lower than that under light irradiation at a wavelength greater than 400 nm. The induction period and the low activities under light irradiation (>420 nm) might be due to the light absorption in the range 400–420 nm of **1**-grafted TiO_2, as shown in Figure 5a. In control experiments under irradiation at a wavelength greater than 400 nm, no reactions were observed when K-**1**, anatase TiO_2, a mixture of $H_3PW_{12}O_{40}$ (5.6 μmol) and TiO_2 (1.0 g), tetra-*n*-butylammonium salt of **1** ($[(n\text{-}C_4H_9)_4N]_{14-x}K_x[O\{Re^V(OH)(\alpha_2\text{-}P_2W_{17}O_{61})\}_2]$, abbreviated as TBA-**1**), and TiO_2–N^+ were used as catalysts (Table 2, Entries 4–8). In addition, **1**-grafted amorphous SiO_2 (11 μmol **1** per g of sample, 0.055 μmol **1** per m^2 of amorphous SiO_2) prepared by the same method as that of **1**-grafted TiO_2 (2.2 μmol **1** per g of sample, 0.055 μmol **1** per m^2 of TiO_2) exhibited no reaction (Table 2, Entry 9). In contrast, H_2 evolution from water vapor under light irradiation (>400 nm) was observed when the $[Re^{IV}Cl_6]^{2-}$-grafted TiO_2 (4.4 μmol Re per g of sample) prepared by the same method as that of **1**-grafted TiO_2 (2.2 μmol **1** per g of sample, 4.4 μmol Re per g of TiO_2) was used as a catalyst. An induction period was not observed. After 5 h and 72 h, 53.8 μmol g^{-1} and 225 μmol g^{-1} of H_2 were evolved, respectively. These values are higher than those obtained with **1**-grafted TiO_2 (Table 2, Entry 10). These results suggested that both the rhenium site and TiO_2 support were crucial for hydrogen production from water vapor under the pres-

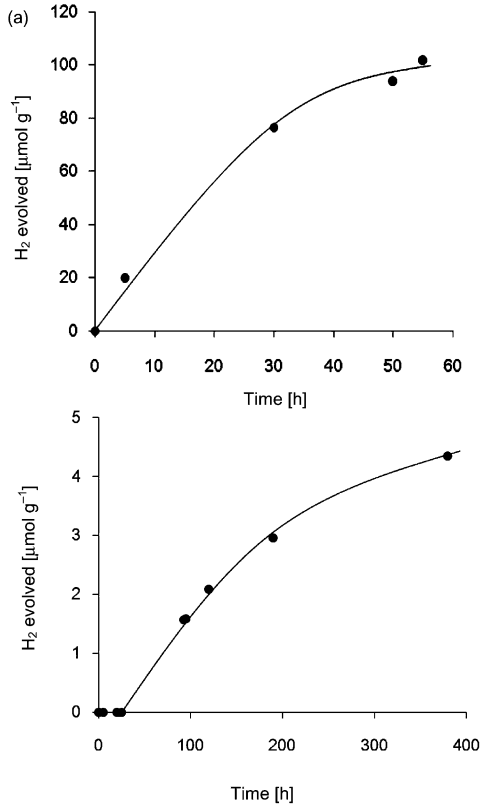

Figure 6. Time course for H_2 evolution catalyzed by **1**-grafted TiO_2 under light irradiation (a) >400 nm and (b) >420 nm. Reaction conditions: see Table 2.

Table 2. Hydrogen evolution from water vapor catalyzed by **1**-grafted TiO_2 under irradiation with visible light.[a]

Entry	Catalyst	Light [nm]	Reaction time [h]	H_2 [μmol g^{-1}]	Rate [μmol g^{-1} h^{-1}][b]
1	**1**-grafted TiO_2	>400	5	19.8	3.96
	(2.2 μmol of **1** per g of sample)		55	101.6	
2	A mixture of **1** and TiO_2	>400	25	2.98	1.19×10^{-1}
	(5.6 μmol of **1** per g of sample)		50	8.52	
3	**1**-grafted TiO_2	>420	93	1.57	1.69×10^{-2}
	(2.2 μmol of **1** per g of sample)		380	4.35	
4	K-**1**[c]	>400	30	n.r.	–
5	TiO_2	>400	30	n.r.	–
6	A mixture of $H_3PW_{12}O_{40}$ and TiO_2	>400	30	n.r.	–
	(5.6 μmol of $H_3PW_{12}O_{40}$ per g of sample)				
7	TBA-**1**[d]	>400	15	n.r.	–
8	TiO_2–N^+	>400	15	n.r.	–
9	**1**-grafted SiO_2	>400	30	n.r.	–
	(11 μmol of **1** per g of sample)				
10	$[Re^{IV}Cl_6]^{2-}$-grafted TiO_2	>400	5	53.8	10.8
	(4.4 μmol of Re per g of sample)		72	225	

[a] Reaction conditions: water (20 Torr; 257.3 μmol), catalyst (500 mg), light (>400 nm and >420 nm), 25 °C. [b] The rate was calculated as H_2 (mol g^{-1}) per reaction time (h). [c] 1 g K-**1** was used. [d] 400 mg TBA-**1** was used.

ent conditions, and the formation of Re^{IV} by the electron transfer reaction of the Re^{V} site in **1**-grafted TiO_2 under light irradiation might accelerate the evolution of hydrogen from water with the decomposition of the surface silane coupling reagent on the TiO_2 support.

When photoreaction of water vapor (20 Torr) was carried out with twice the amount of **1**-grafted TiO_2 catalyst under light irradiation at a wavelength greater than 400 nm, the production of hydrogen in the second run decreased to a third of that in the first run; however, the DR UV/Vis spectrum of the **1**-grafted TiO_2 after the photoreaction (Figure 5b) showed the same spectral pattern as that of the as-prepared **1**-grafted TiO_2. In addition, elemental analysis for the **1**-grafted TiO_2 after the photoreaction revealed that the ratio Re/P was about 1:2. These results suggested that **1** was stable under the present photoreaction conditions; however, the change in the surface structure caused by the decomposition of the surface silane species used as an electron donor might influence the catalytic activities.

To prevent the decomposition of the surface silane coupling reagent of **1**-grafted TiO_2, the liquid-phase photoreaction of water (10 mL) in the presence of $Na_2H_2EDTA{\cdot}2H_2O$ (111 mg, 30 mM) as a sacrificial reagent was repeated three times with the same **1**-grafted TiO_2 catalyst under light irradiation (>400 nm). For the first run, 5.80 μmol g^{-1} and 19.6 μmol g^{-1} of H_2 were produced after 2 h and 4 h, respectively. In contrast, hydrogen production in the second run was increased to 62.5 μmol g^{-1} and 131 μmol g^{-1}, respectively, and the amounts of hydrogen produced were almost the same in the third run (60.5 μmol g^{-1} and 111.1 μmol g^{-1}, respectively). The DR UV/Vis spectrum of the **1**-grafted TiO_2 after the third photoreaction (Figure 5c) also showed the same spectral pattern as that of the as-prepared **1**-grafted TiO_2. These results suggest that neither the surface polyanion **1** nor the surface silane coupling reagent of **1**-grafted TiO_2 were decomposed in the presence of a sacrificial reagent. The lower activities in the first run relative to those in the second and third run might be due to the different adsorption state of water molecules on the surface of the catalyst under the present liquid-phase reaction conditions.

With regard to the reaction mechanism, the excitation of Re^{V} to Re^{V}* by irradiation with visible light and electron transfer from Re^{V}* to Re^{IV} might occur with the decomposition of the surface silane coupling reagent on TiO_2 in the absence of a sacrificial reagent.[19] In addition, the multielectron collection and transfer for the reduction of H^+ to H_2 were performed by TiO_2. Further studies regarding the reaction mechanism are in progress.

Conclusions

The synthesis and crystal structure of a Dawson-type dirhenium(V)-oxido-bridged polyoxotungstate is presented. We have successfully obtained black-purple single crystals of the water-soluble potassium salt $K_{14}[O\{Re(OH)(\alpha_2\text{-}P_2W_{17}O_{61})\}_2]{\cdot}21H_2O$ by treating $[Re^{IV}Cl_6]^{2-}$ with a monolacunary Dawson polyoxoanion. The characterization of compound K-**1** has been accomplished by X-ray structure analysis, elemental analysis, TG/DTA, and UV/Vis absorption, FTIR, ESR, and solution ^{31}P NMR spectroscopy. The crystal structure of K-**1** reveals that the dimeric dirhenium(V)-oxido-bridged structure has overall C_{2h} symmetry. Polyoxoanion **1** was grafted onto the TiO_2 surface by electrostatic binding to give anatase TiO_2 functionalized by a cationic ammonium moiety. Elemental analysis indicated that the seven potassium counterions of K-**1** were ion-exchanged with seven cationic ammonium moieties to form $\{TiO_2\}_{5500}[{\equiv}Si(CH_2)_3N(CH_3)_3Cl]_7[{\equiv}Si(CH_2)_3N^+(CH_3)_3]_7$-$(K_7[O\{Re(OH)(\alpha_2\text{-}P_2W_{17}O_{61})\}_2]^{7-})$ (**1**-grafted TiO_2) and seven molecules of KCl. DR UV/Vis spectrum of **1**-grafted TiO_2 exhibited two sharp bands at 496 nm and 751 nm, which suggests that **1**-grafted TiO_2 absorbs visible light. With the **1**-grafted TiO_2, the hydrogen evolution from water vapor under visible light irradiation (>400 nm and >420 nm) was achieved. To the best of our knowledge, the Dawson dirhenium(V)-oxido-bridged POM $[O\{Re^{V}(OH)(\alpha_2\text{-}P_2W_{17}O_{61})\}_2]^{14-}$ is the first example of the use of a POM as a visible-light-response photocatalyst.

Experimental Section

Materials: $K_{10}[\alpha_2\text{-}P_2W_{17}O_{61}]{\cdot}19H_2O$ was prepared as described in the literature.[20] The number of solvated water molecules was determined by TG/DTA analysis. All the reagents and solvents were obtained and used as received from commercial sources.

Instrumentation/Analytical Procedures: Elemental analyses were carried out by Mikroanalytisches Labor Pascher (Remagen, Germany). The samples were dried at room temperature at 10^{-3}–10^{-4} Torr overnight before analysis. The microanalysis of Re an K elements was specially ordered for the **1**-grafted TiO_2 sample. Infrared spectra were recorded with a Jasco 4100 FTIR spectrometer by using KBr disks at room temperature. Thermogravimetric analysis (TGA) and differential thermal analysis (DTA) data were performed with a Rigaku Thermo Plus 2 series TG/DTA TG 8120 instrument. TG/DTA measurements were performed in air with a temperature ramp of 4 °C per min between 20 and 500 °C. The $^{31}P\{^1H\}$ NMR (161.70 MHz) spectra in solution were recorded in 5-mm-outer-diameter tubes with a JEOL JNM-EX 400 (Kanagawa University) and a JEOL ECA-600 (Shizuoka University) NMR spectrometer. The $^{31}P\{^1H\}$ NMR spectra were referenced to an external standard of 25% H_3PO_4 in H_2O or 85% H_3PO_4 in a sealed capillary. Chemical shifts were reported as negative on the δ scale with resonances upfield of H_3PO_4 (δ = 0 ppm). Solution UV/Vis spectra and diffuse reflectance (DR) UV/Vis spectra were recorded with a Jasco V-570 spectrophotometer. For the DR UV/Vis measurement, a Jasco diffuse reflectance attachment was used. Specific surface areas were measured by the BET method by using an ASAP 2010 (Shimadzu) instrument. X-band EPR spectra were recorded with a JEOL JES-RE Series EPR spectrometer at room temperature.

Synthesis and Characterization of K-1: A mixture of K_2ReCl_6 (0.701 g, 1.47 mmol) and $K_{10}[\alpha_2\text{-}P_2W_{17}O_{61}]{\cdot}17H_2O$ (7.14 g, 1.47 mmol) in water (80 mL) was heated at reflux for 30 min in air. During the refluxing, the color of the solution became a dark purple-black. The solvent was removed by rotary evaporation at 50 °C. The sample obtained was dissolved in hot water (ca. 9 mL) at 80 °C

and placed in a refrigerator to yield a purple-black precipitate, which was collected on a membrane filter (JG, 0.2 μm), and washed with ethanol (3 × 20 mL) and ether (3 × 20 mL). Yield: 6.38 g (89.7%). For $K_{14}[O\{Re^{V}(OH)(\alpha_2\text{-}P_2W_{17}O_{61})\}_2]\cdot 6H_2O$, $H_{14}K_{14}O_{131}P_4Re_2W_{34}$ (9404.277): calcd. H 0.15, Cl 0, K 5.82, P 1.32, Re 3.96; found H 0.13, Cl < 0.1, K 5.91, P 1.24, Re 3.93. A weight loss of 2.8% (from K-**1**) was observed during the course of drying at room temperature at 10^{-3}–10^{-4} Torr overnight before analysis, suggesting the presence of 15–16 weakly solvated or adsorbed water molecules. TG/DTA data: a weight loss of 3.93% was observed below 500 °C; calcd. 3.91% for $x = 21$ in $K_{14}[O\{Re^{V}(OH)(\alpha_2\text{-}P_2W_{17}O_{61})\}_2]\cdot xH_2O$. IR (KBr): $\tilde{\nu}$ = 1091, 1018, 954, 907, 787, 527 cm^{-1}. ^{31}P NMR (in D_2O, at 25 °C, referenced to 25% H_3PO_4): δ = –12.38, –13.39 ppm. ^{31}P NMR (in D_2O, at 25 °C, referenced to 85% H_3PO_4): δ = –12.06, –13.05 ppm. UV/Vis (water): λ (ε, $L\,mol^{-1}\,cm^{-1}$) = 254 (9.39×10^4), 298 (6.28×10^4), 496 (6.61×10^3), 737 (4.02×10^3) nm. ESR (20 °C): silent.

Crystallization of K-1: The sample (1.0 g) was dissolved in aqueous HCl solution (pH = 1.5; 3 mL) at >90 °C, and the purple-black crystals were obtained by slow evaporation at 25 °C in the dark for 6 d. ^{31}P NMR (D_2O, 25 °C): δ = –12.46, –13.45 ppm. For $K_{14}[O\{Re^{V}(OH)(\alpha_2\text{-}P_2W_{17}O_{61})\}_2]\cdot 6H_2O$, $H_{14}K_{14}O_{131}P_4Re_2W_{34}$ (9404.277): calcd. H 0.15, Cl 0, K 5.82, P 1.32, Re 3.96; found H 0.17, Cl < 0.1, K 6.19, P 1.28, Re 4.00.

X-ray Crystallography: Crystals of compound K-**1** were surrounded by liquid paraffin to prevent their degradation. The crystal size was 0.13 × 0.06 × 0.01 mm. Data collection was carried out with a Bruker SMART APEX CCD diffractometer at 90 K. The intensity data were automatically corrected for the Lorentz and polarization effects during integration. The structure was determined by direct methods (SHELXS-97),[21] followed by the subsequent difference Fourier calculation, and refined by the full-matrix least-squares procedure (SHELXL-97).[22] Absorption correction was performed with SADABS (empirical absorption correction).[23] For complex **1**, 34 tungsten atoms, two rhenium atoms, and four phosphorus atoms were clearly identified. Thus, the main feature of the molecular structure of the polyoxometalate was clarified. However, the resolution obtained for the structure of the salt was limited by the poor quality of the available crystals and by the considerable disorder of the countercations and the solvent of crystallization. These features are common in polyoxometalate crystallography.[24]

Crystal Data for K-1: Triclinic space group $P\bar{1}$, purple-black granular crystals, a = 12.663(5) Å, b = 12.824(5) Å, c = 25.348(9) Å, α = 92.348(7)°, β = 103.666(7)°, γ = 114.919(6)°, and Z = 1. The data were collected with a Bruker SMART APEX CCD sealed-tube diffractometer with Mo-K_α (0.71073 Å) radiation [temperature = 90(2) K] in the range $0.84 < \theta < 28.41°$. The final cycle of refinement, including the atomic coordinates, anisotropic thermal parameters (all W, Re, P, K atoms), and isotropic thermal parameters (all O atoms) converged at R_1 = 7.23% and wR_2 = 15.87% ($F_o > 2\sigma F_o$). Further details of the crystal structure investigation may be obtained from the Fachinformationszentrum Karlsruhe, 76344 Eggenstein-Leopoldshafen, Germany [Fax: +49-7247-808-666], e-mail: crysdata@fiz-karlsruhe.de, on quoting the depository number CSD-416410 for K-**1**.

1-Grafted TiO_2: TiO_2 (anatase, 40 $m^2\,g^{-1}$) was pretreated by being dried in the oven (at 50 °C) overnight. The dried TiO_2 support (2.0 g) was dispersed in methanol (160 mL) at 25 °C. A 50% methanol solution of $(MeO)_3Si(CH_2)_3N(CH_3)_3Cl$ (556 μL; 1.0 mmol) was added to this. This mixture was heated at reflux for 6 h at 85 °C. The obtained white powder was collected on a membrane filter (JG, 0.2 μm), washed with methanol (25 mL × 3), and then dried in the oven (at 50 °C) overnight (TiO_2–N^+ was obtained). TiO_2–N^+ [1.5 g, 31.7 μmol of $\equiv Si(CH_2)_3N(CH_3)_3Cl$ groups per g] was suspended in water (45 mL) for 10 min at 25 °C. Solid K-**1** (1.0 g, 0.10 mmol) was added to this suspension. The resulting mixture was stirred at 25 °C overnight. The solid product was collected on a membrane filter (JG, 0.2 μm), washed with water (25 mL × 3), and then dried in the oven (at 50 °C) overnight. [Note: if the **1**-grafted TiO_2 sample was contaminated by K-**1** after the washing with water, the catalytic activity decreased.] Yield: 1.38 g. For $[(TiO_2)_{5500}][Si(CH_2)_3N(CH_3)_3]_4Cl]_7[Si(CH_2)_3N(CH_3)_3]_7(K_7[O\{Re^{V}\text{-}(OH)(\alpha_2\text{-}P_2W_{17}O_{61})\}_2])\cdot(H_2O)_{200}$ (2.2 μmol of **1** per g): calcd. C 0.22, H 0.14, K 0.06, Re 0.08, Si 0.09, Ti 58.00, found C 0.41, H 0.20, K 0.032, Re 0.025, Si 0.16, Ti 58.2. DR UV/Vis spectrum in the visible region: 496, 751 nm. BET surface area: 39.4 $m^2\,g^{-1}$.

Catalytic Reaction Experiments: H_2 evolution from water vapor was carried out at 25 °C. A catalyst (500 mg) was placed into a glass reaction vessel, which was connected to a conventional Pyrex closed gas circulation system (238.8 cm^3). Water vapor (20 Torr; 257.3 μmol) was introduced after evacuation at 25 °C, followed by irradiation with a 500-W Xe lamp equipped with a cut-off filter ($\lambda > 400$ nm and $\lambda > 420$ nm). H_2, O_2, CO, and CH_4 were analyzed by GC (TCD, Molecular Sieve 5A stainless steel columns), and water and CO_2 were analyzed by GC (TCD, Porapak Q stainless steel columns), and assignments were made after comparing these with the authentic samples analyzed under the same conditions. D_2, H_2, and HD were detected with a quadruple mass spectrometer (Pheiffer Vacuum Prisma QME200). The AQY, defined by the following equation, was measured by using combined band-pass and cut-off (Kenko) filters and a photodiode (PM3; COHERENT). AQY = (number of reacted electrons)/(number of incident photons) × 100 = (number of evolved H_2 molecules × 2)/(number of incident photons) × 100.[25]

Supporting Information (see also the footnote on the first page of this article): bond lengths, bond angles, and bond valence sums for compound K-**1** (Tables S1 and S2).

Acknowledgments

C. N. K. is grateful for the support of the IZUMI Science and Technology Foundation, and the Grant-in Aid for Young Scientists (B) from the Ministry of Education, Culture, Sports, Science and Technology, Japan. K. N. acknowledges the support of the Grant-in Aid for Scientific Research (C) No. 18550062 and a High-tech Research Center Project, both from the Ministry of Education, Culture, Sports, Science and Technology, Japan. W. M. acknowledges the support of a High-tech Research Center Project from the Ministry of Education, Culture, Sports, Science and Technology, Japan. The research was partially carried out by using an instrument at the Center for Instrumental Analysis of Shizuoka University. We thank Prof. S. Naito (Kanagawa Univ.) and Dr. T. Miyao (Kanagawa Univ.) for the detection of the D_2 produced from D_2O vapor.

[1] A. Fujishima, K. Honda, *Nature* **1972**, *238*, 37–38.
[2] S. U. M. Khan, M. Al-Shahry, W. B. Ingler Jr., *Science* **2002**, *297*, 2243–2245.
[3] M. Matsuoka, M. Kitano, M. Takeuchi, M. Anpo, J. M. Thomas, *Top. Catal.* **2005**, *35*, 305–310.
[4] Z. Zou, H. Arakawa, *J. Photochem. Photobiol. A: Chem.* **2003**, *158*, 145–162.
[5] I. Tsuji, H. Kato, H. Kobayashi, A. Kudo, *J. Am. Chem. Soc.* **2004**, *126*, 13406–13413.

[6] X. Sun, K. Maeda, M. Le Faucheur, K. Teramura, K. Domen, *Appl. Catal. A: General* **2007**, *327*, 114–121.

[7] a) M. T. Pope, *Heteropoly and Isopoly Oxometalates*, Springer-Verlag, Berlin, **1983**; b) M. T. Pope, A. Müller, *Angew. Chem. Int. Ed. Engl.* **1991**, *30*, 34–48; c) M. T. Pope, A. Müller (Eds.), *Polyoxometalates: From Platonic Solids to Anti-Retroviral Activity*, Kluwer Academic Publishers, Dordrecht, The Netherlands, **1994**; d) *Chem. Rev.* **1998**, *98*, 1–390 (special issue on polyoxometalates; guest editor: C. L. Hill).

[8] S. Anandan, M. Yoon, *J. Photochem. Photobiol. A: Chem.* **2003**, *160*, 181–184.

[9] A. Venturelli, M. J. Nilges, A. Smirnov, R. L. Belford, L. C. Francesconi, *J. Chem. Soc., Dalton Trans.* **1999**, 301–310.

[10] W. J. Randall, T. J. R. Weakley, R. G. Finke, *Inorg. Chem.* **1993**, *32*, 1068–1071.

[11] a) C. Tessier, F. D. Rocon, A. L. Beauchamp, *Inorg. Chem.* **2002**, *41*, 6527–6536; b) S. Fortin, A. L. Beauchamp, *Inorg. Chem.* **2000**, *39*, 4886–4893; c) G. Battistuzzi, A. B. Corradi, D. Dallari, M. Saladini, R. Battistuzzi, *Polyhedron* **1998**, *18*, 57–63 ; d) B. Machura, J. O. Dziegielewski, R. Kruszynski, T. J. Bartczak, J. Kusz, *Inorg. Chim. Acta* **2004**, *357*, 1011–1022.

[12] J. M. Botha, A. Roodt, J. G. Leipoldt, *S. Afr. J. Chem.* **1995**, *48*, 120–126.

[13] H. Sugimoto, T. Takahira, T. Yoshimura, M. Shiro, M. Yamasaki, H. Miyake, K. Umakoshi, Y. Sasaki, *Inorg. Chim. Acta* **2002**, *337*, 203–211.

[14] W. A. Hermann, H. Ding, F. E. Kühn, W. Scherer, *Organometallics* **1998**, *17*, 2751–2757.

[15] F. Ortéga, M. T. Pope, H. T. Evans Jr., *Inorg. Chem.* **1997**, *36*, 2166–2169.

[16] F. Ortéga, M. T. Pope, *Inorg. Chem.* **1984**, *23*, 3292–3297.

[17] C. N. Kato, A. Tanabe, S. Negishi, K. Goto, K. Nomiya, *Chem. Lett.* **2005**, *34*, 238–239.

[18] J. Jarupatrakorn, T. D. Tilley, *J. Am. Chem. Soc.* **2002**, *124*, 8380–8388.

[19] a) H. Hori, K. Koike, *Energy Fuels* **2005**, *19*, 2209–2213; b) E. Amouyal, *Sol. Energy Mater. Sol. Cells* **1995**, *38*, 249–276.

[20] D. K. Lyon, W. K. Miller, T. Novet, P. J. Domaille, E. Evitt, D. C. Johnson, R. G. Finke, *J. Am. Chem. Soc.* **1991**, *113*, 7209–7221.

[21] G. M. Sheldrick, *Acta Crystallogr., Sect. A* **1990**, *46*, 467–473.

[22] G. M. Sheldrick, *SHELXL-97, Program for Crystal Structure Refinement*, University of Göttingen, Germany, **1997**.

[23] G. M. Sheldrick, *SADABS*, University of Göttingen, Germany, **1996**.

[24] a) K. Nomiya, M. Takahashi, K. Ohsawa, J. A. Widegren, *J. Chem. Soc., Dalton Trans.* **2001**, 2872–2878; b) T. J. R. Weakley, R. G. Finke, *Inorg. Chem.* **1990**, *29*, 1235–1241; c) Y. Lin, T. J. R. Weakley, B. Rapko, R. G. Finke, *Inorg. Chem.* **1993**, *32*, 5095–5101; d) T. Yamase, T. Ozeki, H. Sakamoto, S. Nishiya, A. Yamamoto, *Bull. Chem. Soc. Jpn.* **1993**, *66*, 103–108; e) K. Nomiya, M. Takahashi, J. A. Widegren, T. Aizawa, Y. Sakai, N. C. Kasuga, *J. Chem. Soc., Dalton Trans.* **2002**, 3679–3685.

[25] I. Tsuji, H. Kato, H. Kobayashi, A. Kudo, *J. Phys. Chem. B* **2005**, *109*, 7323–7329.

Received: October 17, 2007
Published Online: May 30, 2008

